Hydrol. Earth Syst. Sci. Discuss., 4, 475–521, 2007
www.hydrol-earth-syst-sci-discuss.net/4/475/2007/

Hydrology and Earth System Sciences Discussions

Papers published in *Hydrology and Earth System Sciences Discussions* are under open-access review for the journal *Hydrology and Earth System Sciences*

Modelling the water budget and the riverflows of the Maritsa basin in Bulgaria

E. Artinyan[1], F. Habets[2], J. Noilhan[2], E. Ledoux[3], D. Dimitrov[1], E. Martin[2], and P. Le Moigne[2]

[1]NIMH-regional centre, 139 Ruski blvd., Plovdiv, Bulgaria
[2]Météo-France/CNRM, 42 Coriolis ave., 31057 Toulouse, France
[3]ENSMP/CIG, 35 St Honoré st., 77305 Fontainebleau, France

Received: 8 December 2006 – Accepted: 15 February 2007 – Published: 1 March 2007

Correspondence to: E. Artinyan (eram.artinian@meteo.bg)

Abstract

A soil-vegetation-atmosphere transfer model coupled with a macroscale distributed hydrological model was used in order to simulate the water cycle for a large region in Bulgaria. To do so, an atmospheric forcing was built for two hydrological years (1 October 1995 to 30 September 1997), at an eight km resolution. It was based on the data available at the National Institute of Meteorology and Hydrology (NIMH) of Bulgaria. Atmospheric parameters were carefully checked and interpolated with a high level of detail in space and time (3-h step). Comparing computed Penman evapotranspiration versus observed pan evaporation validated the quality of the implemented forcing. The impact of the human activities on the rivers (especially hydropower or irrigation) was taken into account. Some improvements of the hydrometeorological model were made: for better simulation of summer riverflow, two additional reservoirs were added to simulate the slow component of the runoff. Those reservoirs were calibrated using the observed data of the 1st year, while the 2nd year was used for validation. 56 hydrologic stations and 12 dams were used for the model calibration while 41 rivergages were used for the validation of the model. The results compare well with the daily-observed discharges, with good results obtained over more than 25% of the rivergages. The simulated snow depth was compared to daily measurements at 174 stations and the evolution of the snow water equivalent was validated at 5 sites. The process of melting and refreezing of snow was found to be important on this region. The comparison of the normalized values of simulated versus measured soil moisture showed good correlation. The surface water budget shows large spatial variations due to the elevation influence on the precipitations, soil properties and vegetation variability. An inter annual difference was observed in the water cycle as the first year was more influenced by Mediterranean climate, while the second year was characterised by continental influence. Energy budget shows a dominating sensible heat component in summer, due to the fact that the water stress limits the evaporation. This study is a first step for the implementation of an operational hydrometeorological model that could be used for

real time monitoring and forecast the water budget and the riverflow of Bulgaria.

1 Introduction

In recent years, water related problems and their management appear to be increasingly important in Bulgaria. This is caused partially by drought periods experienced since 1994, but also by the recent inundations and the economic changes. The transition of the country towards a market economic model focuses the attention on a more efficient water use, flood forecasting and mitigation. This increased interest requires more detailed and better founded information in order to provide good support for the decision making system. The needs cover large number of fields: flood prevention, water availability for the industry, agriculture and cities, water quality management, ecology and climate change. Until now the water budget of the country was mostly studied by using statistical and climatologic approaches. That made it possible to estimate the water budget components for each climatic region of the country. The capacity of this approach however is too limited to offer the level of detail that is necessary for real time evaluation of the surface and groundwater resources.

This paper presents the first attempt to implement a soil-vegetation-atmosphere-transfer scheme (SVAT), coupled with a distributed macroscale hydrological model and driven by observed atmospheric forcing for a large region of Bulgaria. The objective of this coupled model is to improve the estimation of the surface water budget (evaporation, soil moisture and runoff) consistently with the simulation of the riverflows. Particularly important is to analyse the partition of precipitation into runoff and evaporation based on a realistic description of the land surface conditions (topography, vegetation, soil).

The study is based on the application of the coupled soil-biosphere-atmosphere (ISBA) surface scheme (Noilhan and Planton, 1989) and the MODCOU macroscale hydrological model (Ledoux et al., 1989) which were already applied on three basins in France: the Adour/Garonne basin (Habets et al., 1999a; Morel, 2003), the Rhone

basin (Habets et al., 1999b; Etchevers et al., 2000), and Seine basin (Rousset et al., 2004). This paper describes the first application for a region that experiences both continental and Mediterranean climates, with pronounced dry period in the summer. This allows validating the functioning of the coupled model in different climatic and land cover conditions. After a description of the hydrometeorological characteristics of the Maritsa basin, the ISBA-MODCOU model is presented. The implementation of the hydrological model and modelling results are analysed in the two last sections.

2 Description of the Maritsa basin: hydrology and meteorological conditions

2.1 Geographic and climatic characteristics

The Maritsa river basin with its tributaries Tundzha and Arda occupies about one third of the surface of Bulgaria – 34 169 km^2. The studied basin includes a small part on Turkish territory down to the town of Edirne, where two important subbasins (of Arda and Tundzha rivers) reach the main river (Fig. 1) and so the total surface in question becomes 36 255 km^2. Within Bulgarian borders, the river length is approximately 320 km with an average slope of 7.7%. It crosses the border between Bulgaria and Greece and after that, until it reaches the Aegean Sea, the river serves as a natural borderline between Greece and Turkey. Therefore Maritsa basin is an important water source in South-Balkan peninsula, passing through three countries. The elevation of the Maritsa watershed goes up to 2925 m at the peak of Musala in the Rila mountain. The main geographical structures are the Thracian Valley in the centre, a part of the Balkan mountains (Stara Planina) at the North and the Rila and Rhodopy ranges in the Southwest (Fig. 1). The average slope of the Bulgarian part of the basin is 12.5%.

Mediterranean influence prevails in the Southeast, where the maximum of precipitation comes in winter. In the central and northern part of the domain the maximum of precipitations occurs in May-June, due to the continental climate influence.

Annual crops (cereals, vegetables, cotton, and tobacco) and orchards are mainly

cultivated in the valleys. The hilly areas are used as a pasture, vineyards or to cultivate potatoes. Forests cover about 40% of the watershed surface. Oak prevails in the valley forests while beech and pine dominate the mountain areas.

2.2 Brief description of the hydrological regime of the surface water and the aquifers

The snowfall in the mountain regions constitutes 30% to 50% of total precipitation. Snow cover lasts 73 to 170 days, for the Rhodopy, Stara Planina and Rila mountains (Vekilska and Kalinova, 1978). According to the climatology the mean annual water budget of the whole country is as follows: precipitations – 690 mm, runoff – 176 mm and evaporation 514 mm (Zyapkov, 1982). The annual averaged streamflow of the Maritsa river varies between 40 m^3s^{-1} and 190 m^3s^{-1} for the period from 1936 to 1975. During the summer, the streamflows are very low. Between July and September, the dams and the ground-water outflows mainly sustain the riverflows.

Unconfined aquifers are another specific feature of the studied area. The larger aquifer is situated in the Upper Thracian Valley. It covers an area of about 6710 km^2 (Kalinova, 1982) between the three main mountain ranges. This aquifer is widely used for irrigation, industrial and domestic water supply. The average outflow of the main aquifer is about 12 m^3s^{-1} while its total storage is about 10.9×10^9 m^3. In the valleys of Kazanlak and Sliven, other smaller basins have total reserves near about 1.14×10^9 m^3 and 0.740×10^9 m^3 respectively (Antonov and Danchev, 1980).

Many karstic areas affect the streamflow in the Rhodopy Mountain. They have well-developed system of underground flow, caves and emerging springs (Fig. 2). For the period 1980–1996, the average discharge of the four biggest springs, Kleptuza, Beden, Devin and Tri Voditzi are respectively 0.40, 0.69, 0.53 and 1.12 m^3s^{-1} (Machkova and Dimitrov, 1990). Those perched mountainous (karstic) aquifers are partially contributing to the main water table in the Upper Thracian Valley, especially from the northern slopes of Rhodopy Mountain. The average annual underground transfer to the plain aquifer is evaluated to 12×10^6 m^3, while 47×10^6 m^3 are emerging at the surface as springs (Troshanov, 1992).

2.3 Anthropogenic influence

During the years between 1950 and 1970 more than fifteen dams were built in the southern part of the country for better control of the riverflow. The total capacity of the main reservoirs is higher than 2810×10^6 m^3 and their overall surface is larger than 12 800 km^2. Although few of them serve as inter-annual flow regulators, usually they hold the peak flow in the winter-spring seasons and release water to produce energy and for irrigation in the summer. Most often the dams are built on the riverbed but in few cases, they are in derivations. Figure 2 shows the location of the main dams in the basin. Other main anthropogenic influence is the direct use of water from the river for irrigation. There are also cases of transferring water from one river basin to another. For example, after the Koprinka dam on the Tundzha River, a catchment takes water for irrigation and hydropower producing purposes and transfers it into the basin of Sazliika river that is not tributary of Tundzha River. Figure 3a presents the effect of different cases of anthropogenic influence on the riverflow for the period 11/1995 to 10/1996. The most important impact is a result of the dams' water storage and release. From June to November the dams contributions represents from 1% to 33% of the riverflow while in January, February and April they store 25 to 27% of the streamflow. Although their annual balance is compensated, they play a considerable role in the monthly partition of the riverflow. For the same period, the water used for irrigation is about 12 mm that is almost 7% of the riverflow. The amount of water transferred from other basins is about 4% of the streamflow. The overall monthly impact of human influence on the natural streamflow for the period 11/1995 to 10/1996 is shown in Fig. 3b. Section 4.2 provides details on the implementation of the anthropogenic influence in the simulation.

3 The ISBA-MODCOU model

3.1 Description of ISBA land surface scheme

The ISBA surface scheme was developed for the climate, mesoscale and prediction atmospheric models used at Météo-France. It represents the main surface processes in a relatively simple way: it solves one energy budget for the soil and vegetation continuum, and uses the force-restore method to compute energy and water transfers in the soil. The two soil layers representation is used – a shallow surface and a root zone (Fig. 4). Four components are used to compute the evaporation: interception by the foliage, bare soil evaporation, transpiration of the vegetation, and sublimation of the snowpack.

Two fluxes of water in the soil are computed: a surface runoff (Q_r) and drainage (D)(Fig. 4). Subgrid heterogeneities of the soil moisture are involved only in the surface runoff. To evaluate the subgrid runoff, the concept of the Variable Infiltration Capacity (VIC) (Dûmenil and Todini, 1992) is used. It considers that a fraction of the cell is saturated, and thus, can produce surface runoff, even if the whole mesh is not saturated. Such fraction is almost zero when the soil is dry (around the wilting point), and is going up to 100% when the whole cell is saturated. It is varying according to an exponential function, which is based on a shape parameter (b).

In this application, the snow pack is represented by one layer with uniform temperature, density and water content (Douville et al., 1995).

3.2 Description of the conception of additional reservoirs for the drainage flow

The previous applications of the coupled ISBA-MODCOU model were done for relatively wet regions, without pronounced dry periods. In the case of the Maritsa river during the dry period of the year the runoff is mostly sustained by the deep soil drainage and the water table, where it exists. The process occurring in the unsaturated zone, between the soil root-zone and the water table, has a high contribution to the total

runoff especially in the summer. In the two-layer soil scheme, used in this application, water transfer in the unsaturated zone was not implemented. For better simulation of the observed time delay in the streamflow, two additional reservoirs were introduced, between the surface scheme ISBA and the MODCOU hydrological model (Fig. 4). In the mountain area, where aquifer layer does not exist, only these additional reservoirs simulate the time lag of the drainage water during the transfer in the unsaturated zone. In this new module, a fraction α of the gravitational drainage simulated by ISBA (D) is transferred to the first reservoir. This reservoir has a water content h_1 and a depletion coefficient C_1 that is relatively low in order to induce large time delay. When its maximum level $h_1$max is reached, water surplus is transferred to the second reservoir. This second reservoir represents the less compact and more fissured upper area of the geological profile. Therefore it has a higher depletion coefficient C_2, leading to a shorter time delay. When the second reservoir level h_2 reaches its maximum – $h_2$max, the extra water leaves the reservoirs. Thus, the drainage part of the runoff is formed by Eq. (1) and (2):

$$Q_d = D \times (1 - \alpha) + Q_{ov} + h_1 \times C_1 + h_2 \times C_2 \quad (1)$$

$$\text{With} \quad Q_{ov} = D \times \alpha - (h_2 \max - h_2) \quad (2)$$

Therefore the five parameters of the additional reservoirs are:
α – coefficient controlling the drainage water input into the reservoirs
$h_1$max, $h_2$max – maximum levels of the reservoirs
C_1, C_2 – depletion coefficients of the reservoirs, $C_1 \leq C_2$

Q_d is transferred either to the riverflow where there is no aquifer or to the water table simulated by MODCOU. The part of it that passes through the first reservoir ($h_1 \times C_1$)could be considered as the slower part of drainage. The additional reservoirs are processed at the time step and using the grid of the hydrological model. The higher resolution of the hydrological grid gives the possibility to calibrate the parameters by nested subbasins, which is described in Sect. 5.2. Parameters variability could be

related to the geomorphic characteristics (elevation, slope) or to the geologic profile, if such information is available.

3.3 Description of MODCOU

The macro-scale hydrological model MODCOU was used in various applications (Ledoux et al., 1989). MODCOU takes into account the surface and underground layers. The surface routing network is computed starting with the topography, by using a geographical information system. The surface and underground domains are divided into grid cells of embedded size (from 1 to 4 km), the higher resolution being associated to the river grid cells. The transfer time between two grid cells is based on the topography, the distance between the cells and the surface of the basin. The surface runoff computed by ISBA is routed to the river network and then to the river gages using isochronous zones with a daily time step. The drainage computed from ISBA and from the new drainage module contributes to the evolution of the groundwater table, which evolves according to the diffusivity equation. Exchange of water between the groundwater table and the river are computed according to simple relations (Ledoux et al., 1989). At the end, the flows from the surface layer and from the groundwater table form the riverflow at the gauging stations.

4 Implementation of ISBA-MODCOU in the Maritsa basin

4.1 Hydrological parameters

The hydrographical surface network as well as the underground layer grid was established by using a GIS based on the topography (Golaz et al., 2001). For that purpose, the GTOPO30 database (provided from USGS EROS Data Centre) was used. The grid consists of 11 661 meshes in the surface layer, including 2387 river cells; and 4390 cells for the underground layer (Fig. 2).

A maximum transfer time Tc for the water to reach the outlet was established for the Maritsa basin, according to the observed streamflow: Tc=6 days. The evolution of groundwater table is controlled by transmissivity and storage coefficients. They were calibrated for eight subregions of the unconfined underground layer. The existing publications were used to estimate a first guess of these coefficients. Transmissivity varies from 1.0×10^{-3} to $34\times10^{-3}\,m^2s^{-1}$ while the values of the storage coefficient are between 0.20 and 0.23 (Antonov, 1980).

The five additional parameters of drainage reservoirs had to be calibrated for each of the 68 subwatersheds

4.2 Implementation of dam reservoirs in the simulation

Data about the water budget of twelve reservoirs and about water redirecting and channelling were collected for the first year of simulation. They were used for the calibration period, first, to validate the simulated streamflow at the dam entrance and, second, to impose the dam release to the simulated streamflow after the dam.

In the simulation, all the streamflows that are downstream the dams or the redirecting points were corrected in order to take into account the impact of the constructions along the riverflow. This correction was achieved by considering the time lag implied by the storage and the transfer in the channel. Natural riverflows of Maritsa river (8 gages), Tundzha river (2 gages), Chepinska river (2 gages), Vacha river (4 gages), as well as the Arda river outlet were corrected, by subtracting the simulated natural flow coming from the rivercells just upstream the dams, and by adding the observed dams' water release while respecting the time lag between the two cells. In the northern part of the basin, the observations showed that the outflows from irrigation dams did not sustain the riverflow in summer. Instead of that, those outflows were redirected through irrigation channels (Fig. 3a). Therefore, this part of the streamflow (11.7 mm or 7%) was subtracted from the simulated streamflow. At the basin level, the overall effect of anthropogenic influence for the period 1 November 1995 to 30 October 1996 was about −4 mm, and near 7 mm was transferred from other basins (Fig. 3a).

4.3 Surface parameters

The ISBA parameters can be determined by the soil texture and the vegetation maps using tables of correspondence, as detailed in Noilhan and Lacarrere (1995).

The vegetation map compiled by Champeaux and Legléau (1995) from the NDVI archive distinguishes 12 vegetation types. The resulting vegetation map (Fig. 5) shows that forests are the dominant vegetation type in the mountains. In the valley, Crop (3) – that is interpreted as Mediterranean region cereal, associated with dry summer conditions, is dominant. The Rock type influences few grids in the high mountain area of Rila and Stara Planina. A single vegetation class stands for any forest type. The monthly evolution of leaf area index (LAI), vegetation cover (VEG), and roughness length ($z0_v$), were related to the 2 years' satellite archive of the advanced very high resolution radiometer/normalized difference vegetation index (AVHRR/NDVI), following the method presented in Habets et al. (1999a). The minimum surface resistance (R_{sm}) and albedo (α_v) are constant in time and linked to the vegetation type.

In the study detailed maps of the soil properties - the percentage of sand and clay as well as the soil depth linked to the maximum depth of the root system of cultivated crops by agricultural region were established (Trendafilov, 1996[1]). These maps were used to obtain data at 1 km resolution. The soil depth map was compared to the soil depths derived from the vegetation type. The last one gives more than 150 cm depth for the forested area, which is not realistic for the mountain forests in Bulgaria (Ninov, 1982). The soil depth used in this study varies between 40 cm and 150 cm. Only the forested regions in the valley have deeper soil – 180 cm.

The calibration of the b parameter used in the subgrid runoff scheme was performed by using the same ideas as in Dûmenil and Todini (1992). It depends on the altitude,

[1]Trendafilov, Ch.: Maps of soil mechanical properties in the region of Maritsa river basin, personal archive of the author, 1996.

as presented in Eq. (3),

$$b = \left(0.2 + \frac{Alti}{3000}\right) \times 1.4, \quad (3)$$

with *Alti* is the cell elevation [m] and $0.28 \leq b \leq 1.68$.

Equation (3) gives the best modelling results for high flow conditions. The values of b are significantly higher than the values calibrated in preceding application (Artinian, 1996). This result is explained with the introduction of additional reservoirs for the drainage flow, as now the efficient simulation of peak flows needs lowering of the precipitation's fraction transferred to drainage reservoirs.

4.4 Atmospheric forcing

4.4.1 Meteorological database

To compute the water and energy cycle the ISBA surface scheme needs 8 atmospheric parameters: rainfall and snowfall, air temperature and humidity at 2 m, wind velocity, atmospheric pressure, global and atmospheric radiations. For the application over France, the SAFRAN analysis system is used (Quintana Seguì et al., 2007[2]). Such analysis system was not yet implemented in Bulgaria, and thus, an important work was done in order to generate the atmospheric database.

Such database was assembled for 26 months (from 1 August 1995 to 30 September 1997). The following data sources were available at the National Institute for Meteorology and Hydrology of Bulgaria (NIMH): 12 synoptic stations, recording atmospheric parameters each 3 h; 55 climatologic stations with 3 values a day – at 07:00, 14:00 and 21:00 h LT and 175 precipitation stations – measuring the daily precipitation and snow depth (Tables 1 and 2). For the first year snow density data of five additional stations

[2]Quintana Seguì, P., Le Moigne, P., Durand, Y., Martin, E., Habets, F., Baillon, M., Franchisteguy, L., Morel, S., and Noilhan, J.: The SAFRAN atmospheric analysis, Description and validation, Journal of Applied Meteorology and Climatology, under review, 2007.

were available. The global solar radiation data were obtained from two stations, one in the valley close to the town of Chirpan and the second one in a mountain location at 1800 m a.s.l. Data with 3-h step was taken from monthly paper reports. The continuous records of global radiation of Chirpan station were obtained on graph paper strips – one per day. These analogous records were scanned and hourly sums were computed by integration. The atmospheric forcing was prepared at a 3-h timestep; while the precipitations were collected on a daily basis. To be consistent with the density of the observation network and the hydrological grid, an 8×8 km grid cell was used to interpolate in space the atmospheric forcing. This meteorological grid consists of 638 cells (Fig. 2). Next two sections present the preparation of the atmospheric parameters needed for the modelling.

4.4.2 Snow and rain precipitation, air temperature, wind velocity and specific air moisture fields

In order to select only realistic data, a criterion based on the standard deviation (σ) was used to isolate erroneous data. It reflects the variability of a parameter around its average value for certain periods so that errors in data series of relatively high homogeneity, as air temperature, relative humidity and wind velocity should be easily detected. However, it can't be used to estimate the errors in precipitation data series. Air temperature, wind velocity and relative moisture records were carefully checked and corrected using the $\pm 3 \times \sigma$ rejection criterion. The precipitation data were checked by comparison with the climatological maps of precipitation for a given season (Hershkovich et al., 1982).

The point scale observations were interpolated in space using two software packages. The spatial interpolation of the temperature was made with software dedicated to scattered data, statistically linked to the topography, the Aurelhy method (Benichou and Le Breton, 1987). However, when the temperature field is not enough correlated to the elevation, due to atmospheric temperature inversion that appears most often in winter time, the krigging software Bluepack was preferred. This method leads to acceptable results, with higher quality than Aurelhy.

The temperature observations come from two meteorological networks with different time steps of observations (climatological and synoptic). The first one has higher detail in space, while the second is more detailed in time. To produce temperature forcing with good resolution both in space and time, we combined the two fields in one new field using a spline function that approximates the daily temperature variability. The same method was used to work out the field of the relative air moisture, needed to compute the specific air humidity. The other atmospheric fields (wind velocity, rain and snow precipitation) were interpolated with the Bluepack krigging software.

The interpolation of precipitation is difficult because of its high spatial variability. Where the rain gauges are too close, the Bluepack krigging method gives noisy results. Noise analyse showed that it depends on the average distance between two stations for the whole field. That brought the idea of "averaging neighbours" method: where the distance between two precipitation stations is less than the required minimum, the average of the observed values of the two gauges is attributed to both stations before the interpolation. For the Rhone basin precipitation field, the minimum tolerable distance was 2 km (Artinian, 1996). In the case of the Maritsa river basin, where the rain gauges are scarce, this distance was determined to be 6 km.

Surface atmospheric pressure was estimated directly from the elevation because the variability due to the topography is several times higher compared to the seasonal one.

Specific humidity of the air at 2 m was calculated using values of the atmospheric pressure, temperature and relative humidity of the air.

4.4.3 Atmospheric radiation and global radiation fields

To compute the atmospheric radiation the formula of Staley and Jurica (1972) was used. It takes into account the air temperature, air specific humidity and cloudiness.

For the global radiation, few observations were available: only two stations had measured directly the global radiation at a hourly time step: Chirpan in the plain (173 m) and Rozhen in the mountain (1750 m). Measurements of the bright sunshine hours were made at 15 sites, using a sunshine recorder, which allows the estimation of the

"bright sunshine ratio" i.e., the ratio of the actual bright sunshine to potential bright sunshine. Also, cloudiness was observed at 55 sites.

Global radiation depends on the elevation, because of the impact of the aerosol concentration on the atmospheric transmittance (Hottel, 1976) and air turbidity. To take into account such impact, as well as all the available data, we used a modified version of the parameterisation suggested by Kasten and Czeplak (1979). It is based on a statistical relation between the hourly global radiation, the hourly bright sunshine ratio, and the 3-hourly cloudiness, observed at the different sites. It is expressed as follows (Eq. 4)

$$Rg = Rg_0 \times \left\{ A_1 \times \left(1 - 0.88 \left(\frac{Nb}{10} \right)^{3.5} \right) + B_1 \times \frac{Alti}{1000} + C_1 \times Sun \right\} \quad (4)$$

where Rg stands for the hourly global solar radiation (Wm^{-2}), Rg_0 stands for theoretical clear-sky global radiation computed according to the solar elevation angle at sea level (Kasten and Czeplak, 1979), Nb stands for the average hourly cloudiness (varying from 0 to 10), *Alti* stands for the altitude of the grid point (m), *Sun* stands for the hourly bright sunshine ratio, ranging from 0 to 1 and A_1, B_1, C_1 – are empirical coefficients

The empirical coefficients A_1, B_1 and C_1 were found to depend on the value of Rg_0, so they were established for 10 intervals of Rg_0. These coefficients, when computed for the entire range of Rg_0 between 0 and 900 Wm^{-2} were: A_1=0.288, B_1=0.196 and C_1=0.691.

The atmospheric parameters were computed for two hydrologic years – 1995/1996 and 1996/1997. The maps of the atmospheric forcing for the two years are presented in Fig. 6. It shows the annual accumulated total precipitation, snowfall, mean annual air temperature and global solar radiation for the two years of simulation. There is a large spatial variability. The total precipitation is marked by strong values in the mountain areas, but the higher values for the second year are situated in the Southeast, where the more pronounced Mediterranean climate can produce intense rainfall. In the valley the annual value of total precipitation varies from 400 to 600 mm, while in the mountains

it varies from 700 to 1300 mm. Snowfall is more important in the mountain. It varies from 10 mm in the valley to 800 mm in the Rila Mountain.

4.4.4 Validation of the atmospheric forcing

As all the available data were used to establish the atmospheric forcing, it is not possible to validate it directly. However, indirect validation can be made, by using pan evaporation observations. Pan evaporation depends on the atmospheric conditions. It can then be compared to pan evaporation computed from the new data set. Such comparison relies on the hypothesis that the pan evaporation is comparable to the Penman potential evapotranspiration. The accumulated Penman evaporative demand of the atmosphere (Choisnel, 1988) was computed, at a 10-day timestep, by using the interpolated values for temperature, radiation and wind speed, and compared (Fig. 7) to the pan evaporation observed at 5 sites. The coefficient of determination of the comparison is R^2=0.87 and the root mean squared error $RMSE$=5.3 mm.

5 Modelling results

5.1 Hydrological database and methodology

The hydrological database consists of daily streamflow discharge of 56 river gages. The inflow and release flows data of 12 dams, as well as snow density measurements only for the first year from the National Electricity Company (*NEK*); and from the Water Management Company (*Vodno Stopanstvo*) for the northern part of the basin were obtained (Table 2). From the total number of 68 stations and dams, only 41 could be used for statistical comparisons, because for 10 stations and 12 dams no data was available for the validation year. Additionally, five small catchments (smaller than 50 km^2) were discarded from the comparison because there was a 10% error between the reported surface of the subbasin and the modelled one. In order to check the quality of the

simulation, three statistical criteria were computed for each gauging station: the ratio between simulated and observed annual discharge *Qsim*/*Qobs*, the daily efficiency *E* (Nash and Sutcliffe, 1970), and the coefficient of determination – R^2. To achieve perfect simulation these three statistical numbers should be equal to 1.0. The ratio *Qsim*/*Qobs* gives an estimation of the annual partitioning of the precipitation into runoff and evaporation, whereas R^2 indicates if the simulated and the observed streamflow are significantly correlated. The efficiency E is an intermediate criterion, very sensitive to the flood overestimation.

In the following sections, the method of calibration of the unsaturated reservoirs is presented, and the results in terms of streamflow, snow height, soil moisture, and water and energy budgets are discussed.

5.2 Calibration of the unsaturated zone reservoirs

The calibration method is a multiple step optimisation procedure based on the statistical results of the comparison between simulated and observed streamflow. First, the extreme limits of the parameters were set. For each subbasin, the total volume of the runoff for the dry period of the year – *Qdry* [mm] was computed. This first guess value is assumed to be close to the average level h_1 of the first reservoir. The initial estimation of the extreme values for the parameter $h_1$max where chosen to be $10 \times Qdry \geq h_1 \text{max} \leq \frac{1}{4} \times Qdry$. The limits for the depletion coefficient C_1 were deducted from extreme values of $h_1$max in order to simulate the average daily streamflow during dry periods. The parameter $h_2$max was initialised with the same extreme levels. To initialise the parameter C_2, we used the relations $C_1 < C_2$ and $C_2 < 0.20$, as with the value of 0.2 a reservoir of $h_2$max=300 mm (maximum value found in the previous step) is depleted in about 5 days. The parameter α varies between 0.0 and 1.0. An iterative procedure was undertaken, with cycles between the extremes for each parameter, using a large step. Each time when the statistics were higher than in the previous step, the resulting combination of parameters was stored. This procedure was repeated with a smaller step by using the parameters already defined in the previous step for

the initialisation. The optimisation process was repeated until the statistics achieved convergence. Table 3 shows the computed average and extreme values of the five parameters.

At the end of the calibration phase, the following results were observed:

- The valley subcatchments present high values of the coefficient: α=0.80 to 1.0, which means that only small part of the streamflow is a rapid flow.
- The Southeast part of the basin (Arda and tributaries) shows low rate of drainage water storage: α=0.05 to 0.35.
- The subcatchments from regions with pronounced karst development in the Rhodopy Mountain show higher α coefficient: α=0.75 to 1.0 than the other catchments with the same average elevation (α=0.1 to 0.65).

These observations correspond to some published results about the partition of the runoff according to its origin – surface, drainage and deep drainage (Yordanova, 1978). However, in many cases the lack of knowledge about the anthropogenic activity leads to errors during calibration. In order to estimate the parameters with high quality, detailed information about human activity in the studied area is necessary.

5.3 Results in term of streamflow simulation

For the entire studied area, the error on the mean annual discharge for the first (calibration) year is lower than 20% for half of the stations. On average, the annual simulation for the calibration year is close to the observations for the main stations (overestimation of 13%). The observed and simulated daily streamflow discharges for 8 river gages are given (Fig. 8). Their positions are shown in Fig. 2.

The value of E is greater than 0.7 for 27% of the stations and greater than 0.6 for 36% of them. The best values are obtained for the main rivers (Fig. 8a to d and Table 4).

For the calibration year, as it could be expected, better results are obtained when the dam inflow/outflow are taken into account (Table 4), except for the annual ratio

Qsim/*Qobs* that is overestimated. This overestimation is due to the underestimation of the fraction of the dam water release that is used for irrigation purposes. This amount should be removed from the simulated riverflow. The influence of imposed streamflow is stronger near to the dams (for instance at Plovdiv) and diminishes downstream (for instance at Svilengrad). It rises again at the outlet (Edirne) because of the proximity to the Arda river reservoir cascade.

The lowest efficiencies are computed for the Northwest part of the Tololnitza and Striama watersheds, where the rain gauges are too few.

For the second validation year (1996/1997) the efficiency is lower. The value of E is higher than 0.6 for 32% of the stations, but the error on mean annual discharge remains at the same level – lower than 20% for half of the stations. Twelve gauging stations, not perturbed by dams, have higher statistic results for the validation year than for the year of calibration.

5.4 Snow simulation

To validate the snow cover evolution simulated by the ISBA surface scheme, 20 climatological stations were selected according to the following criteria: minimum elevation 450 m, more than 100 days of observed snow cover for the two years, observations available for the entire simulation period and grid cell altitude close to the station's elevation (difference lower than 200 m). At these sites, the interpolated air temperature is closer to the observed one comparing to sites with only rain/snow measurement stations. The mean evolution of snow depth for these stations is depicted in Fig. 9a and b. The second year, the results are poorer and one of the reasons for this is the generally higher temperature in the winter of 1997 (on average for January 1996 it is -1.64°C; while for January 1997 it is $+2.01^{\circ}$C). Therefore the melting of snow pack during the day and the refreezing of the liquid water stored in the snow pack at night happens more often during the second year than the first one. Such a process is not taken into account in the one-layer snow scheme used in this study. It was however simulated by the 3 layers snow schemes recently developed for ISBA (Boone and Etchevers, 2001),

and the application of that scheme showed good results for both years. The RMSE for the daily snow depth for the first year of the simulation for these sites is 5 cm but for the second simulated year it is 13 cm. Observations of the snow pack from 174 stations at a daily step were considered in order to evaluate the quality of snow simulation at the basin-range. A comparison between the averaged observed and simulated snow depth for 174 stations is presented in Fig. 9d. This scatter plot shows the snow scheme efficiency but the result is highly influenced by the quality of air temperature interpolation, which is steady in the neighbourhood of the 55 climatological stations.

Snow density together with snow depth data is available for five sites and only for the first modelled winter – 1995/96. The snow density and snow water equivalent (*SWE*) were compared after averaging the results of corresponding model grid cells and the daily data of five measuring sites (Fig. 9c).

The model simulates well the snow height and the corresponding water content in cold conditions (T°C<0.0). In case of rainfall over the snow pack (T°C>0.0), and periods of melting-freezing, the *SWE* is strongly underestimated. This is leading to a lower *SWE*, than the observed one, during the less cold period. As mentionned the snow scheme efficiency was improved with the 3-layer snow scheme of ISBA developments not used in that study.

5.5 Soil moisture simulation

In order to validate the model soil moisture simulation agro-meteorological data were collected from 10 stations measuring the soil water content (Table 5).

The measurements of volumetric soil moisture were available from ten agro-climatic stations, each one with three profiles. Agrometeorologists systematically selected the three profiles of each site with different vegetation cover – one with wheat or barley vegetation (winter crops), one with perennial vegetation (ex. vineyard, rose, etc.) and one with annual vegetation (cotton, lucerne or corn). The measurements were made by weighting the soil sample, extracted three times a month, before and after drying. No measurements were made during the winter season. The soil and vegetation char-

acteristics observed in situ and those used in the simulation for the ten sites are given in Table 5.

The soils in Bulgaria's valley have often high available water capacity (*AWC*) (Richards and Wadleigh, 1952). Alluvial meadow soils, for instance, contain high amount of clay – between 40 and 60% and a corresponding high *AWC* e.g. 110 to 180 mm for the top 1 m soil depth (Dimitrova, 1991), especially where the humus content increases. *AWC* computed by ISBA (75 to 90 mm) are lower than the measurements. To compare the evolution of the observed against the simulated soil water content a normalization of both values was made. Thus, the moisture computed by the surface scheme is normalized by using Eq. (5) and then compared to the normalized measured top 1-m soil moisture. In the last two columns of Table 5 the statistics of the comparison are given.

$$W_n = \frac{w_2 - w_2\,\mathrm{min}}{w_2\,\mathrm{max} - w_2\,\mathrm{min}} \tag{5}$$

where $w_2$min and $w_2$max are the minimum and maximum values of the compared grid cell or respectively the observed soil profile and w_2 is the actual soil volumetric water content (m^3/m^3). The analysis of the measured values showed that all profiles of some sites were highly influenced by irrigation, so these stations were discarded from the comparison. As the winter cereals are less dependent on water supply, they are usually not irrigated. Thus, two kinds of validation were made: the first one used the averaged values of all the soil profiles of the seven not-irrigated sites (21 profiles) and the second one – only the cereal profiles of these sites, i.e. wheat and barley. The comparison showed that for most profiles, the higher and lower values of observed and simulated soil moisture had a good correlation in time. The model simulates fast lowering of the soil moisture in April and May, which corresponds to the seasonal behaviour (in terms of soil moisture usage) of the observed winter crops. The results proved that winter cereals observed in situ were properly defined (in terms of soil moisture usage) by the prescribed vegetation types – Crop (3) and Crop (4), except for the period from June to August when soil moisture was depleted faster in the simulation. Too low prescribed

LAI and *VEG* for those months could be the reason for this overestimation of the bare soil evaporation (*LEG*) (Fig. 11b).

5.6 Water and energy budgets at the basin scale

5.6.1 Surface water budget

Figure 10 shows the annual maps of accumulated evaporation and runoff for the two years of simulation. The fields have large spatial variability.

The total evaporation is linked to the topography. Accumulated annual evaporation varies from 300 to 780 mm. The highest value (780 mm) is simulated the second year in the Rhodopy Mountain. The generally higher values in the mountains are related to the dense forest vegetation, and the more important rainfall at this altitude.

The annual accumulated runoff varies spatially from 15 mm to 580 mm for the first year. During the second year it ranges from 12 to 680 mm. The valleys show the lowest values, while the region of East Rhodopy Mountain is producing systematically the higher runoff. This phenomenon is linked to the combination of several factors: almost no forest, shallow soil and the intense rainfall. While in the forested areas rainfall is subject to retention by the forest litter and the evaporation rate can be high, for the south-eastern part of the Rhodopy mountain flash floods are occurring almost every year. The drainage fraction represents 77% of the runoff for the first year and 74% for the second one – respectively 125 and 126 mm (Table 6). However, almost all of it comes from the mountain area. The drainage in the valley remains very low because of the high evapotranspiration and its contribution to the aquifer is weak. An exception of that could be the deep infiltration fraction of water used for irrigation.

Monthly values of the water budget (Fig. 11a) show that there are three precipitation maximums during the first year: in November-December, in February and in September. For the second year the maximums are in November, March–April and August. The first year is dominated by the Mediterranean climate (with winter precipitations) while the second year is typical for the continental water cycle. The evaporation follows

the temperature variability and the water availability. Thus, it has higher values in April and May (87, 84 mm), for the first year, when the two conditions intervene. It is also linked to the development of vegetation. It rises also in September (61 mm) with the increase of precipitations. The bare ground evaporation (*LEG*) causes the September rise while in the other cases (Fig. 11b) the plant transpiration (*LETR*) represents the larger fraction of the total evaporation. In summer, transpiration is lower (30 and 20 mm) because of the water stress. For the second year the total evaporation (*LE*) is higher by about 100 mm (Table 6), caused by the spring and summer precipitations together with the higher temperatures in that season. The runoff variability is linked to the same processes. When the precipitations occur in winter, they contribute to the runoff because of the low evaporation. In the opposite, huge part of the spring and all the summer precipitations evaporate and do not contribute to the runoff.

The soil water content rises for the first year between October and December, then in February and decreases very fast from March to May (Fig. 11c). For the period from June to September the soil reservoir water content rises with about 100 mm. For the second year the process of replenishment is shorter but more intensive in winter. The depleting occurs one month later due to the spring precipitations. Figure 11c shows that the unsaturated zone reservoir plays an important role on the water budget as well.

The water budget is highly influenced by the contrast between the valley and the mountain areas of the region. However, part of this contrast is hidden by the dams' impact on the runoff. Mountainous catchments are highly influenced by the snowmelt. On the opposite, Arda river and its tributaries, which are under Mediterranean influence, are not affected by snow. Table 6 shows the components of the water budget of four main subbasins and also of four smaller watersheds not disturbed by anthropogenic activity. For the entire basin the relation between evaporation and precipitation (*E/P*) is about 0.7 for the first year and 0.8 for the second. For comparison the mountain catchments (Fig. 8g) have values between 0.6 and 0.65, which is due to the snowmelt feeding and low temperatures. Southeast Rhodopy Mountain tributaries – Vurbitza and Krumovitza rivers (Fig. 8e and f), show lower values of that parameter: 0.43 and 0.51.

The shallow soils, intensive precipitations and the lack of forests in the region explain this phenomenon.

5.6.2 Aquifer water budget

At the basin scale, the water table (plain aquifer) has a relatively small contribution to the runoff. That is partially due to the small amount of infiltration in the area with aquifer layer. As that layer covers the valley where the evapotranspiration takes large part of the precipitations, only small part of the infiltration water reaches the water table. The aquifer maintains the riverflow with 19 $m^3 s^{-1}$, or 6% of the total streamflow, which corresponds to the reported data (Antonov and Danchev, 1980). The recharge occurs mainly in winter and spring months at a rate of 6–7 mm per year. The monthly aquifer budget is positive only for March 1996. The two-year's budget is negative, about −10 mm. This corresponds to a decrease of aquifer level. Recharges by infiltration of irrigation water and lateral underground recharge are not taken into account.

5.6.3 Energy budget

The energy budget is linked to the water budget by the evapotranspiration term and is expressed by the Eq. (6):

$$R_n = H + LE + G \tag{6}$$

where R_n stands for the net radiation flux, H and LE stand for the sensible and latent heat fluxes and G stands for the ground heat flux. The annual variations of these fluxes are driven by the net radiation flux. The monthly budget of the studied area, for the two years of simulation, is presented in Fig. 12a. R_n varies between 15 and 130 Wm^{-2}. The higher values are in June–August – over 115 Wm^{-2} for the two-year simulation, while the lower values are in the period November–February – below 25 Wm^{-2}. The evaporation fluxes varies from 8 to 70 Wm^{-2} between the winter and spring months. The higher values are in spring because the evaporative demand of the atmosphere

coincides with the water availability in the soil. In summer, the latent heat is lower than the sensible heat because of the lack of water for evaporation. During the second year, more water is available in summer and the two main components of the energy budget are closer. The ground heat flux has its maximum values in March–May – 4.3–4.5 Wm^{-2}. The dominating sensible heat flux in summer months is due to two main reasons: the lack of precipitation and the prescribed vegetation type with low values of the vegetation fraction in summer. This leads to heating of the bare ground and consequently with a water stress to reduce evaporation, and increase the sensible heat flux. The Bowen ratio (*H/LE*) for the first year is equal to 1.36 and to 0.92 for the second one. The simulated evolution of the energy budget components is close to the published values for the whole country territory (Vekilska, 1982). The published climatological values of ratio LE/R_n vary between 0.42 and 0.70 (in average 0.46 in the simulation) and the relation H/R_n is between 0.30 and 0.45 (in average 0.52 in the simulation). Finally, the ground heat flux is positive from March to August. Figure 12b shows the above mentioned published values, converted into Wm^{-2}, compared to the modelling results.

6 Conclusion

The purpose of this project was to implement a coupled hydrometeorological model (ISBA-MODCOU) in Bulgaria, in order to study the variability of water and energy budgets.

The hydrometeorological model was already used in France, in association with the SAFRAN atmospherical analysis system. As such system was not available in Bulgaria comprehensive work was done to generate a complete atmospheric database. It has been demonstrated that even with the relatively scarce meteorological network, the available data is qualitatively and quantitatively sufficient for the modelling. However, a huge preparatory work was needed, in order to extract data from various formats, often on paper support, to correct and interpolate the point scale observations.

In order to improve the simulation of the riverflows, a simplified scheme describing the impact of the unsaturated zone was added. It consists of two reservoirs fed by the drainage simulated by ISBA and allows simulation of the time delay for the transfer of water from the soil column to the aquifer or the river. As those reservoirs use the same daily time step than the hydrological model, their five parameters could be calibrated versus the observations, with high spatial resolution and short computing time.

The impact of the numerous dams and pumping the river was quantified thanks to the numerous data collected. Such impact has a clear annual cycle, and, for a given month, it can represent up to 4% of the annual discharge. Due to the precision of the data collected, the effects of the dams on the riverflow could be taken into account in the simulation.

The simulation was made over two annual cycles, and the validation was performed by using observed snow depth, snow water equivalent, daily riverflow, and soil moisture. The simulation was in good agreement with the observations. For instance, more than 25% of the rivergages were simulated with efficiency above 0.7.

The study shows that the country experiences water stress in summer, which limits the evapotranspiration. Indeed, the annual Bowen ratio is rather high –1.36 in 1995–1996 and 0.92 in 1996–1997.

The results of this first application for the Maritsa, Tundzha and Arda basins in Bulgaria will be used in many directions:

- It's a first step for the implementation of an operational hydrological model that could be used for both monitoring and forecast of water budget and riverflow. This is a priority after the inundations in August 2005 and March 2006. These events lead to economical losses of more than 850×10^6€ only in Bulgaria. In time of floods, after crossing the Bulgarian territory, Maritsa and its tributaries Arda and Tundzha rivers cause inundations in Turkey and Greece. Therefore the implementation of an efficient operational hydrological forecasting system in the region will have highly positive cross border impact.

– It allows to define the methodology and to estimate the amount of data needed for a long-term retrospective study. Such study is necessary to understand the characteristics of the water system in Bulgaria, and to be able to anticipate the impact of climatic change.

– To optimise the meteorological and hydrological network in order to reduce their maintenance cost since financial resources for public domain are a major issue.

Acknowledgements. The authors wish to acknowledge the financial support of Météo-France and Ecole Nationale Supérieure des Mines de Paris (ENSMP). The authors would like to express their deep gratitude to all colleagues from GMME/MC2 – division of the National Centre for Meteorological Research of Météo-France (CNRM), to T. Bojkova and the colleagues from NIMH for their suggestions and their help to obtain and prepare the necessary data sets for the performance of this study.

References

Antonov, Ch. and Danchev, D.: Underground waters in Popular Republic of Bulgaria. State Publishing House: Technika, Sofia 1980, 1980.

Artinian, E.: Modélisation hydrologique du bassin du Rhône. ENM, Météo-France, Rapport de mastère, décembre 1996, Toulouse, 1996.

Benichou, P. and Le Breton, Od.: Prise en compte de la topographie pour la cartographie des champs pluviométriques statistiques, in: La Météorologie, 7e série, n 19, octobre 1987, 1987.

Boone, A. and Etchevers, P.: An intercomparison of three snow schemes of varying complexity coupled to the same land surface model: local-scale evaluation at an alpine site, Journal of Hydrometeorology, 4, 374–394, 2001.

Champeaux, J.-L. and Legléau, H.: Vegetation mapping over Europe using NOAA/AVHRR, in: The 1995 meteorological satellite data user's conference, pages 139–143, Winchester, UK, EUMETSAT, 1995.

Choisnel, E.: Estimation de l'évapotranspiration potentielle á partir des donées météorologiques, La Météorologie, 7, 19–27, 1988.

Dimitrova, Yu.: Bulk density and changes depending on the moisture with different mechanical and humus soil composition, Soil science and agrochemistry, XXVI, 3–4, Sofia, 1991.

Douville, H., Royer, J.-F., and Mahfouf, J.-F.: A new snow parameterisation for the Météo-France climate model. Part I: Validation in stand-alone experiments, Climate Dyn., 12, 21–35, 1995.

Dûmenil, E. and Todini, L.: A rainfall-runoff scheme for use in the Hamburg climate model, in: Advances in Theoretical Hydrology, a tribute to James Dooge, edited by: O'Kane, J. P., page 462, McGraw-Hill, New York, 1992.

Etchevers, P., Golaz, C., and Habets, F.: Simulation of the water budget and the riverflows of the Rhone basin from 1981 to 1994, J. Hydrol., 244, 60–85, 2000.

Golaz, C., Etchevers, P., Habets, F., Ledoux, E., and Noilhan, J.: Comparison of two hydrological simulations of the Rhone basin, Phys. Chem. Earth, 26(5–6), 461–466, 2001.

Habets, F., Noilhan, J., Golaz, C., Goutorbe, J. P., Lacarrère, P., Leblois, E., Ledoux, E., Martin, E., Ottlé, C., and Vidal-Madjar, D.: The ISBA surface scheme in a macroscale hydrological model applied to the Hapex-Mobilhy area. Part I : model and data base, J. Hydrol., 217, 75–96, 1999a.

Habets, F., Noilhan, J., Golaz, C., Goutorbe, J. P., Lacarrère, P., Leblois, E., Ledoux, E., Martin, E., Ottlé, C., and Vidal-Madjar, D.: The ISBA surface scheme in a macroscale hydrological model applied to the Hapex-Mobilhy area. Part II: simulation of streamflows and annual water budget, J. Hydrol., 217, 75–96, 1999b.

Hershkovich, E., Stephanov, I., Ganeva, B., et al.: Agro-climatical atlas of Bulgaria, Mean Direction of Hydrology and Meteorology – Bulgarian Academy of Sciences, Institute of Hydrology and Meteorology, Institute of Cartography, Sofia, 1982.

Hottel, H. C.: A Simple Model for Estimating the Transmittance of Direct Solar Radiation Through Clear Atmospheres, Solar Energy, 18, 129, 1976.

Kalinova, M.: Unconfined underground waters, in: Geography of Bulgaria – Physical Geography, 1982: Natural Conditions and Resources, Bulgarian Academy of Sciences, p. 259, Sofia, 1982.

Kasten, F. and Czeplak, G.: Solar and terrestrial radiation dependent on the amount and type of cloud, Solar Energy, 24, 177–189, 1979.

Ledoux, E., Girard, G., and Marsily, G.: Spatially distributed modelling: conceptual approach, coupling surface water and groundwater, in: Unsaturated Flow in Hydrologic Modelling Theory and Practice, edited by: Morel-Seytoux, H. J., by Kluwer Academic Publishers, 1989.

Machkova, M. and Dimitrov, D.: Book of reference for the quantitative characteristics of the underground waters for the period 1980–1996, National Institute of Meteorology and Hydrology, Sofia, 1999.

Morel, S.: Modélisation distribuée du bilan hydrique a l'échelle régionale: application au bassin Adour Garonne, Doctoral Thesis, Toulouse 3 University, 2003.
Nash, J. E. and Sutcliffe, J. V.: Riverflow forecasting through conceptual models, 1, a discution of principles, J. Hydrol., 10(3), 282–290, 1970.
Ninov, N.: Soils in the mountain area in: Geography of Bulgaria – Physical Geography, 1982: Natural Conditions and Resources, Bulgarian Academy of Sciences, 380–388, Sofia, 1982.
Noilhan, J. and Lacarrère, P.: GCM gridscale evaporation from mesoscale modelling, J. Climate, 8(2), 206–223, 1995.
Noilhan, J. and Planton, S.: A simple parameterization of land surface processes for meteorological models, Mon. Wea. Rev., 117, 536–549, 1989.
Richards, L. A. and Wadleigh, C. H.: Soil water and plant growth, in: Soil Physical Conditions and Plant Growth, edited by: Shaw, B. T., American Society of Agronomy Series Monographs Volume II, pp. 74–251, Academic Press, New York, 1952.
Rousset, F., Habets, F., Gomez, E., Le Moigne, P., Morel, S., Noilhan, J., and Ledoux, E.: Hydrometeorological modeling of the Seine basin using the SAFRAN-ISBA-MODCOU system, J. Geophys. Res., 109, D14105, doi:10.1029/2003JD004403, 2004.
Staley, D. and Jurica, G.: Effective atmospheric emissivity under clear skies, J. Appl. Meteor., 11, 349–356, 1972.
Troshanov, N.: Hidden discharge evaluation of the North Rhodopes karstic water to the Upper Thracian lowland, Engineering Geology and Hydrogeology, 22, 10–27, Sofia, 1992.
Vekilska, B. and Kalinova, M.: Snow pack in the West Stara Planina Mountain and its impact on the riverflow, Problems of the Geography of P. R. of Bulgaria 5, Sofia, Nauka i Izkustvo, 1978.
Vekilska, B.: Radiation and heat budget in: Geography of Bulgaria – Physical geography, Natural conditions and resources, 1982, pp 169–171, Bulgarian Academy of Sciences, Sofia, 1982.
Yordanova, M.: Genesis and monthly partition of the riverflow in the East Rhodopy Mountain – a result from the complex effect of the physical and geographical factors, Thesis, Geographical Institute, Bulgarian Academy of Sciences, 1978.
Zyapkov, L.: Water budget of the river basins, in: Geography of Bulgaria – Physical Geography, 1982: Natural Conditions and Resources, p 327, Bulgarian Academy of Sciences, Sofia, 1982.

Table 1. Sources of meteorological data, used for the preparation of model input database, following the station types and the time step of observation. Observers using traditional measurement instruments, except those for global solar radiation, make all the measures. Aurelhy (Benichou and Le Breton, 1987) and Bluepack interpolation packages were available at Météo-France/CNRM.

Data type	Unit	Stations type/amount		Time step of observation		Used software or method for spatial interpolation
		Synoptic	Climatological	Synoptic	Climatological	
Precipitation	[mm]	16	55+120 rain gauges	At 2, 8, 14, 20 h UTC 6-h step	At 7 h LT – daily sum	Bluepack
Air Temperature at 2 m	[°C]	16	55	3-h step	At 7, 14 and 21 h LT	Aurelhy or Bluepack
Wind velocity	[ms^{-1}]	16	55	3-h step	At 7, 14 and 21 h LT	Bluepack
Global Solar radiation	[Wm^{-2}]	2 stations – Chirpan and Rozhen		1 h sum		Function
Sunshine ratio	[1/10]	15		hourly		Function
Cloudiness	[1/10]	16	55	3-h step	At 7, 14 and 21 h LT	Bluepack
Relative humidity	[%]	16	55	3-h step	At 7, 14 and 21 h LT	Bluepack

Table 2. Data collected for the validation of the modelling results: streamflow discharge was computed as daily average value, using hourly recordings or staff gage level observations and rating curves; dam's inflow and release from Northern part of the Maritsa basin were obtained as 10 day accumulated values, while from the southern reservoirs they were more detailed – with daily step; soil moisture was measured as difference before and after drying soil samples extracted 3 times a month; snow water equivalent (*SWE*) was measured at five stations maintained by NEK.

Data type	Unit	Amount of stations	Type of stations	Data time step
Streamflow Discharge	[m^3/s]	56	River gages	Daily
Dam inflow and release	[m^3/s]	12	Reservoir's budgets	Daily and 10 day averages
Soil moisture in the 100 cm column	[mm]	10	Agro-meteorological stations – samples taken the 7th, 17th and 27th day of the month	3 times monthly
Snow depth	[cm]	55+120	Climatological + 120 rain gauges	Daily
SWE	[mm]	5	Climatological	Daily
Pan evaporation	[mm]	5	Climatological	Daily

Table 3. Average and extreme values of the five parameters for the reservoirs representing the unsaturated zone.

Parameter	Average	Maximum	Minimum
α	0.75	1.0	0.05
$h_1$max	60 [mm]	300	5
$h_2$max	90 [mm]	300	1
C_1	4.0×10^{-3}	4.0×10^{-2}	1.0×10^{-4}
C_2	2.5×10^{-3}	0.13	1.0×10^{-4}

Table 4. Comparison statistics of series of simulated against measured daily streamflow discharge for the main river gages on Maritsa and Tundzha rivers and four not perturbed by human activity watersheds: Varbitza, Krumovitza, Chepelarska and Mochuritza. Imposed streamflow takes into account streamflow stored in or released from dam reservoirs, taking water from the river bed and flow redirections. *Qsim*/*Qobs* is the simulated versus observed discharge ratio, E the daily efficiency, and R^2 the coefficient of determination.

			Calibration year with imposed streamflow (1995/1996)			Calibration year without imposed streamflow (1995/1996)			Validation year without imposed streamflow (1996/1997)		
River, Gage station	Basin surf. (km^2)	Avg. altitude (m)	*Qsim*/*Qobs*	E	R^2	*Qsim*/*Qobs*	E	R^2	*Qsim*/*Qobs*	E	R^2
Maritsa, Plovdiv	7926	915	1.10	0.83	0.93	0.94	0.29	0.72	0.87	0.37	0.67
Maritsa, Svilengrad	20840	582	1.04	0.84	0.93	0.96	0.84	0.94	0.91	0.70	0.85
Tundzha, Elhovo	5551	475	1.00	0.64	0.82	1.16	0.47	0.79	0.75	0.54	0.76
Maritsa, whole basin	36255		1.16	0.75	0.95	1.02	0.65	0.88	1.10	0.47	0.86
Varbitza, Djebel	1149	584	0.89	0.77	0.88	0.89	0.77	0.88	0.96	0.78	0.89
Krumovitza, Krumovgrad	468	494	1.10	0.71	0.84	1.10	0.71	0.84	1.31	0.43	0.85
Chepelarska, Narechen	393	1356	1.09	0.72	0.87	1.09	0.72	0.87	0.95	0.59	0.77
Mochuritza, Vodenichene	1110	259	1.38	0.50	0.78	1.38	0.50	0.78	1.06	0.70	0.84
Average			1.09	0.72	0.87	1.07	0.62	0.84	0.99	0.57	0.81

Table 5. Parameters and modelling results for the observed soil-crop profiles. The second and third columns show the type of crops observed in the sites and the prescribed vegetation types used by the model for the corresponding grid cell. Next two columns show the field capacity (*Wfc*) and wilting point (*Wwilt*) (values given for 1 m column depth), as observed and as prescribed in the model. Coefficients of determination of the comparison between simulated versus observed series of normalized soil moisture are given in the last two columns: the first one shows the statistics when all observed crop profiles of the site are considered, while the last column shows the results obtained using only wheat or barley profiles (winter cereals). Plovdiv, Rajevo Konare and Ivailo sites are considered as influenced by irrigation.

Location Soil type	Observed crop types	Prescribed vegetation types aggregation by order of importance in the grid cell	*Wfc* [mm]		*Wwilt* [mm]		Simulation results for the period 95/97	
			Model	Measure	Model	Measure	Avg. R^2	W&B R^2
Sadievo Leached Cinnamonic Forest soil (Alfisol)	Barley Corn Grape	Grassland + Crops (2)	285	349	197	200	0.75	0.81
Liubenova Mahala *Smolnitsa* (Vertisol)	Barley Sunflower	Crops (3)	332	404	244	257	0.68	0.81
	Lucerne			377		231		
Chirpan *Smolnitsa* (Vertisol)	Wheat Corn Cotton	Crops (3)	337	428	249	250	0.54	0.86
Kazanlak Delluvial-meadow (Luvisol)	Wheat Rose	Grassland	212	336	129	144	0.55	0.83
	Mint			336		148		
Haskovo Leached *Smolnitsa* (Eutric Vertisol)	Wheat Sunflower Grape	Crops (3, 4, 2)	315	403	226	256	0.80	0.76
Liubimets Cinnamonic Forest soil (Alfisol)	Wheat Sunflower	Crops (3)	289	382	200	212	0.78	0.77
	Grape			367		125		
Plovdiv Alluvial-meadow (Fluvisol)	Wheat Corn	Crops (3, 4)	245	303	158	175	0.62	0.62
	Apple			389		175		
Rajevo Konare Alluvial-meadow (Fluvisol)	Wheat Sunflower Tobacco	Crops (3, 4, 2)	329	289	241	85	0.32	0.64
Ivailo Cinnamonic Forest soil (Alfisol) – Podzols	Wheat Corn Apple	Crops (3, 4, 2)	235	268	149	141	0.74	0.71
Yambol *Smolnitsa* (Vertisol)	Wheat Corn Lucerne	Crops (3, 4, 2)	337	386	249	207	0.73	0.76

Table 6. Annual water budget for some main gauge stations and four not anthropized watersheds: *Ptot* – total precipitation [mm]; *Psnw* – snow precipitation [mm]; *Etot* – total evaporation [mm]; *Qtot* – total runoff [mm]; *Dw* – evolution of soil water storage [mm]; *Eg* – evaporation from the bare soil [mm]; *Er* – plant interception evaporation [mm]; *Etr* – plant transpiration [mm]; *Es* – sublimation/evaporation at the snow surface [mm]; ISBA drainage *D* and surface runoff *Qr* [mm]; Storage in the snow pack is neglected for all the watersheds as the simulation ends on 30 September, when snow pack rarely exists.

River, (sub-basin)	1995–1996	Surface	*Ptot*	*Psnw*	*Etot*	*Qtot*	*Dw*	*Eg*	*Er*	*Etr*	*Es*	*D*	*Qr*
Maritsa, Edirne (whole basin)		36 255	621	163	433	163	25	177	90	139	26	125	38
Maritsa, Svilengrad		21 379	598	174	430	140	28	174	91	136	29	105	35
Maritsa, Plovdiv		8077	623	211	423	164	36	160	106	116	41	125	39
Tundzha, Elhovo		5549	651	128	484	120	48	193	101	166	24	83	37
Chepelarska, Narechen		412	765	317	460	283	21	149	122	120	70	223	61
Varbitza, Djebel		1144	751	162	381	359	11	167	85	114	15	293	66
Krumovitza, Krumovgrad		531	811	185	368	445	−2	160	77	113	18	365	80
Mochuritza, Vodenichene		1190	680	91	470	140	70	187	84	185	14	97	42
River, (sub-basin)	1996–1997	Surface	*Ptot*	*Psnw*	*Etot*	*Qtot*	*Dw*	*Eg*	*Er*	*Etr*	*Es*	*D*	*Qr*
Maritsa, Edirne (whole basin)		36 255	652	105	513	171	−32	206	97	193	16	126	45
Maritsa, Svilengrad		21 379	603	106	510	125	−32	207	92	193	18	87	38
Maritsa, Plovdiv		8077	595	149	519	112	−36	203	102	184	31	75	37
Tundzha, Elhovo		5549	669	94	572	154	−58	211	109	237	16	109	45
Chepelarska, Narechen		412	900	316	583	341	−25	199	141	170	74	265	76
Varbitza, Djebel		1144	894	83	457	473	−36	193	100	157	6	371	102
Krumovitza, Krumovgrad		531	938	152	404	566	−33	170	86	138	10	453	113
Mochuritza, Vodenichene		1190	654	62	594	139	−79	215	106	266	7	98	42

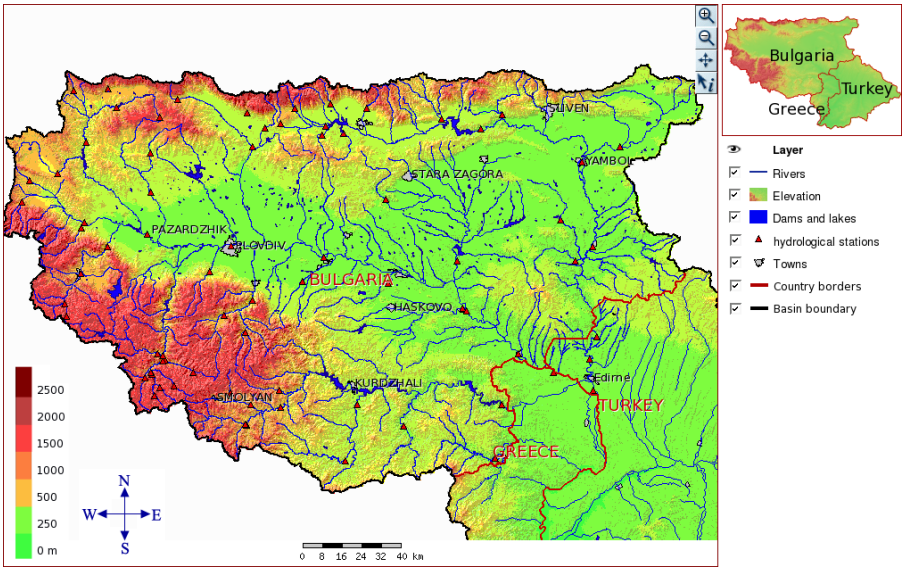

Fig. 1. Map of the Maritsa basin in Bulgaria. The red boundary line represents the political borders between Bulgaria and Turkey, Bulgaria and Greece, Turkey and Greece. The basin border is shown with black line. The modelling area goes down to the town of Edirne in Turkey, where the watersheds of the Arda (from West) and Tundzha rivers (from North) reach the main river course.

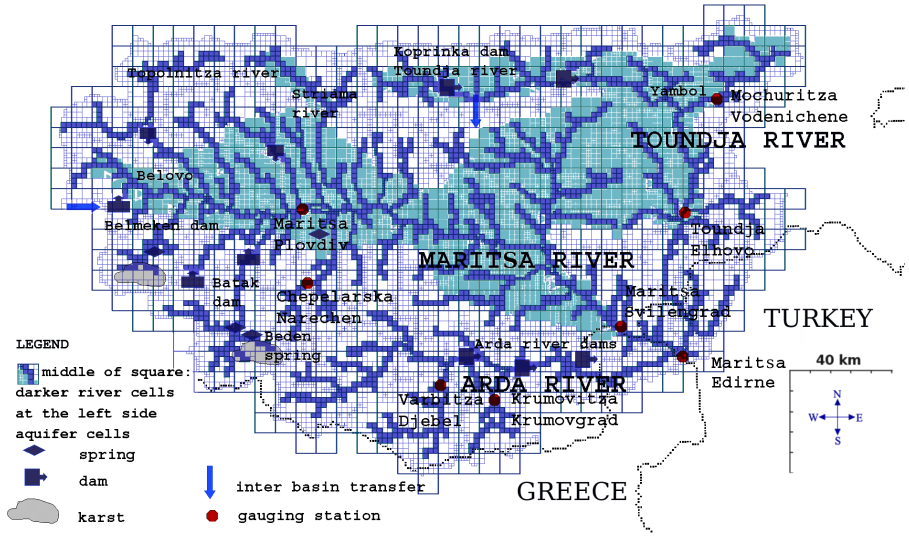

Fig. 2. Surface hydrological network of the Maritsa river system: the river meshes are in dark colour, grey colour represents the aquifer area; dams are shown with dark box; the larger springs with diamond and river gauges with red circles; karstic areas in Maritsa river basin are shown too.

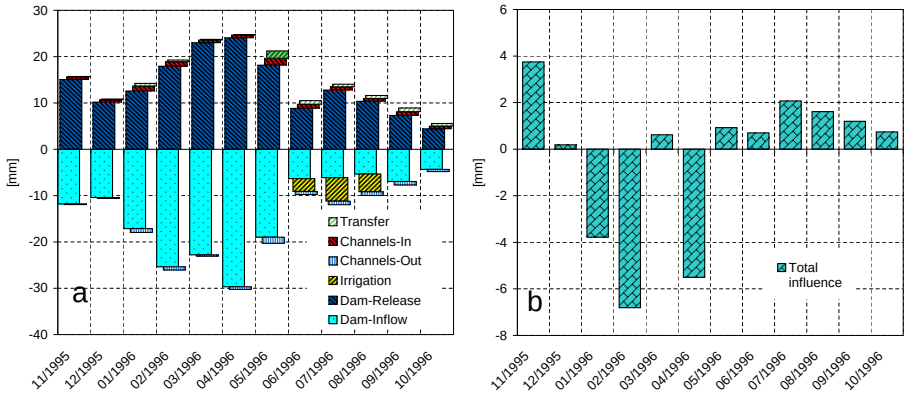

Fig. 3. **(a)** Monthly budget of the anthropogenic influence on natural riverflow for the entire basin in Bulgaria in [mm]. "Dam-Inflow" – the dam reservoirs inflow, "Dam-Release" – the dam reservoirs outflow, "Channels-In" – added water into the riverflow from within Maritsa basin, "Channels-Out" – redirected part of the riverflow within Maritsa basin, "Transfer" – additional water from outside the Maritsa basin, "Irrigation" – water used for irrigation purposes. **(b)** Overall effect of the anthropogenic influence on natural riverflow [mm].

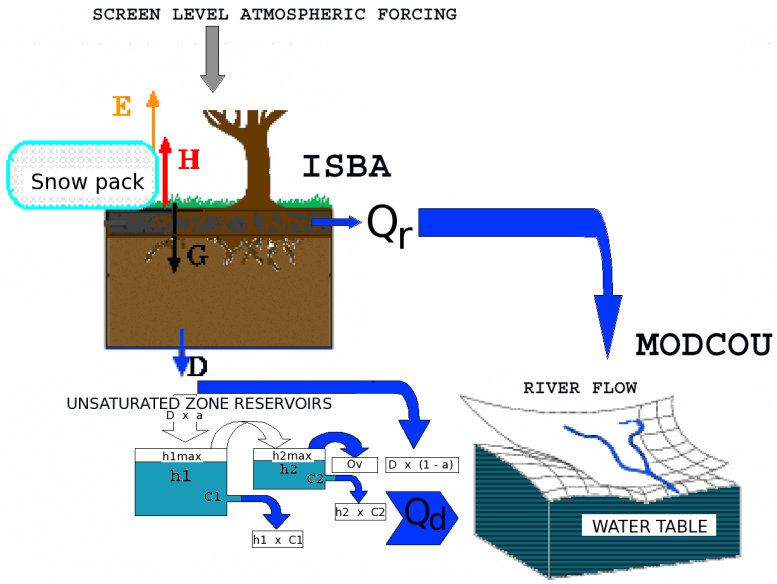

Fig. 4. Scheme of the ISBA – MODCOU coupled model with the 2 additional reservoirs for the drainage, representing the unsaturated layer: *H* – sensible heat flux, *LE* – evaporation (latent heat) flux, *G* – ground heat flux, *D* – ISBA drainage, *Qr* – ISBA surface runoff, *Qd* – final drainage.

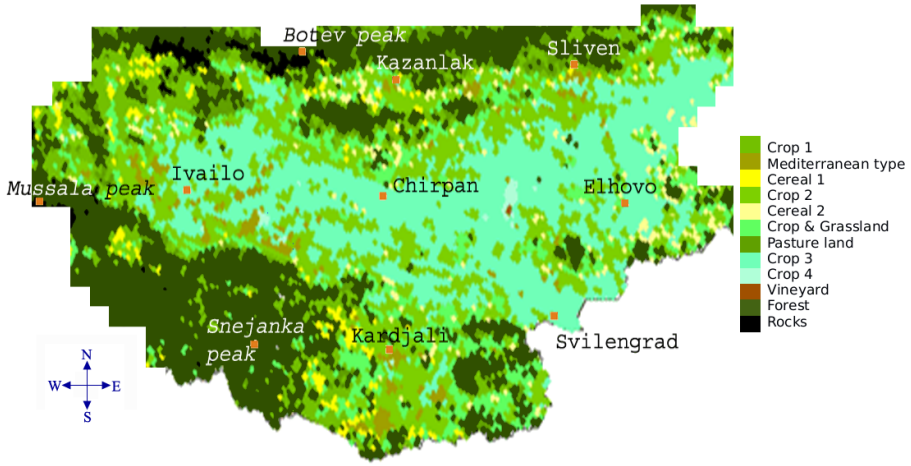

Fig. 5. Map of the dominant vegetation types: forests are dominant in the mountain ranges; crops, and especially crop #3 and #4 – interpreted as Mediterranean cereal, are prevalent in the valley; rocks are appearing close to mountain peaks.

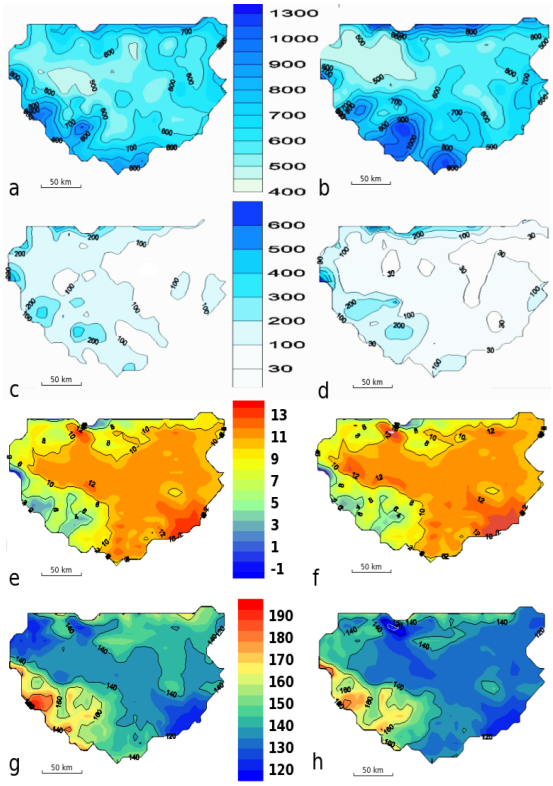

Fig. 6. Annually averaged atmospheric fields for 1996 (left) and 1997 (right). **(a)** and **(b)** Total precipitations [mm]; **(c)** and **(d)** Snow precipitations [mm]; **(e)** and **(f)** Air Temperature at 2 m [°C]; **(g)** and **(h)** Global Radiation [Wm^{-2}].

515

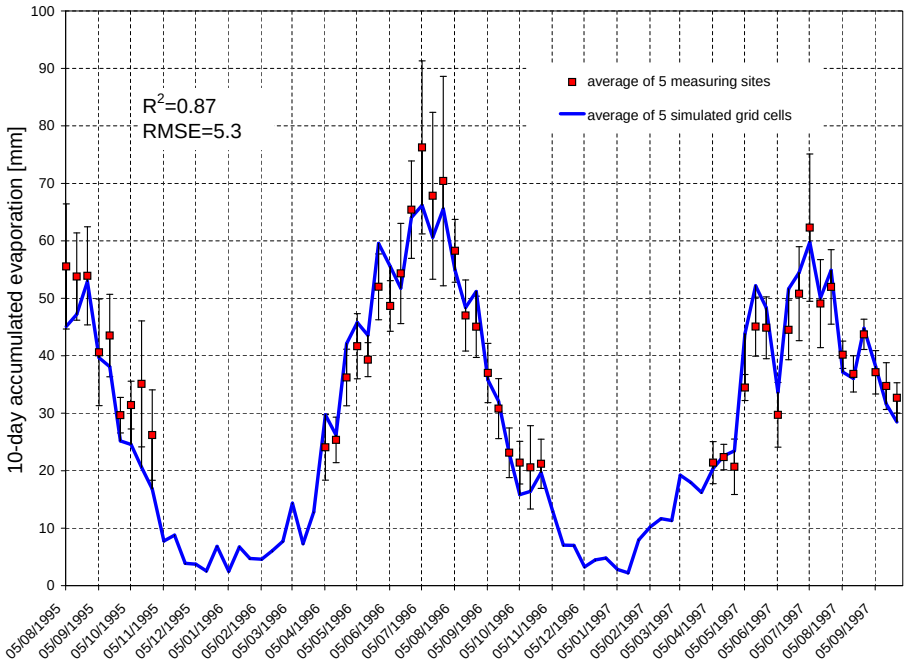

Fig. 7. Series of 10-day accumulated Penman evaporation computed with the model forcing and observed 10 day accumulated pan evaporation [mm]. Each point value is averaged from the observations of five stations or from the corresponding five grid cells values.

516

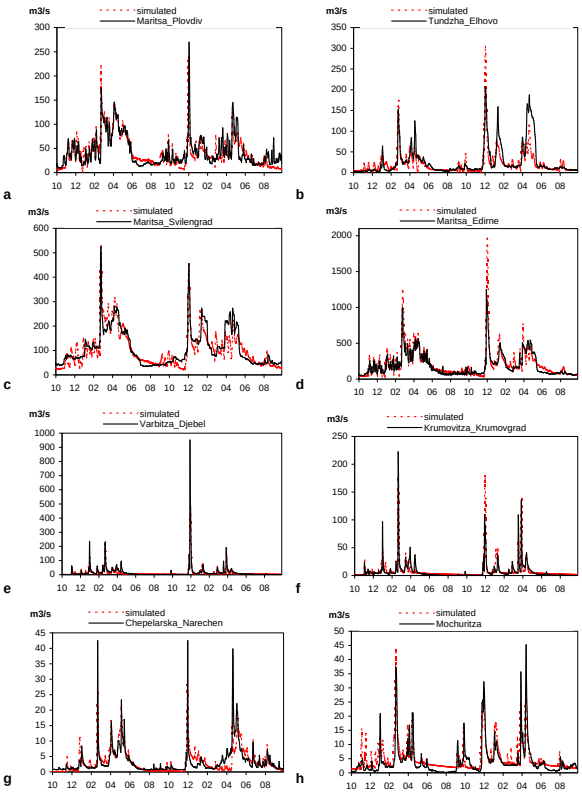

Fig. 8. Comparison of the observed (solid line) and simulated (dashed line) hydrographs for main Maritsa and Tundzha subbasins (**a**, **b**, **c** and **d**) and four watersheds not disturbed by human activities (**e**, **f**, **g** and **h**) for the calibration (1995/1996) and validation (1995/1996) hydrological years.

517

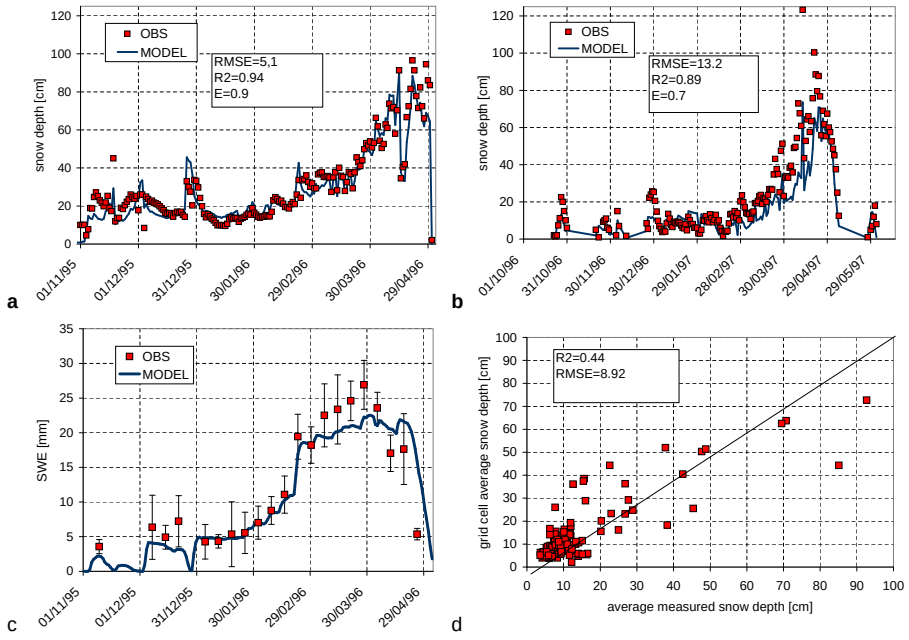

Fig. 9. Snow depth and snow water equivalent (*SWE*) comparisons: Comparison of the averaged on 20 points of the observed and simulated snow depth [cm] – **(a)** winter 1995/1996; **(b)** winter 1996/1997; **(c)** Comparison of the averaged on 5 sites (*SWE*) observed and simulated [mm] **(d)** Scatter plot of the average simulated snow depth [cm] compared to the average observed snow depth for the whole observation network (174 gauges).

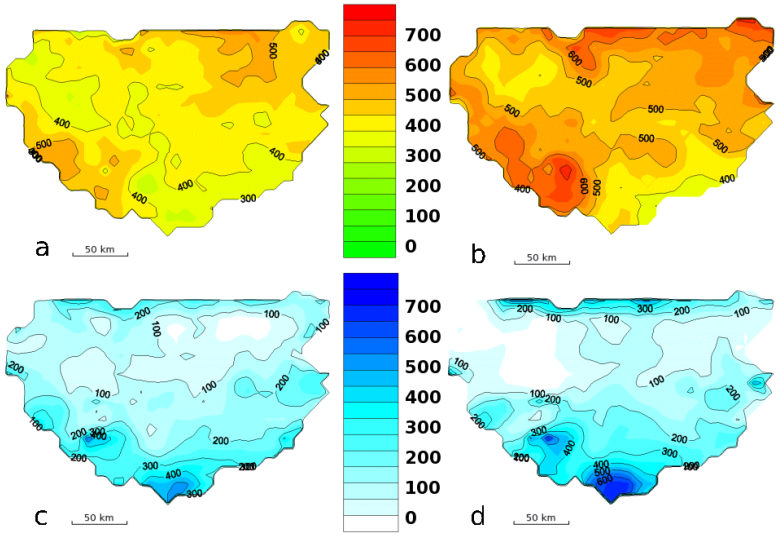

Fig. 10. Annually accumulated fields for the water budget components to the left for 1995/1996 and to the right for 1996/1997: **(a)**–**(b)** Total evaporation [mm]; **(c)**–**(d)** Runoff [mm].

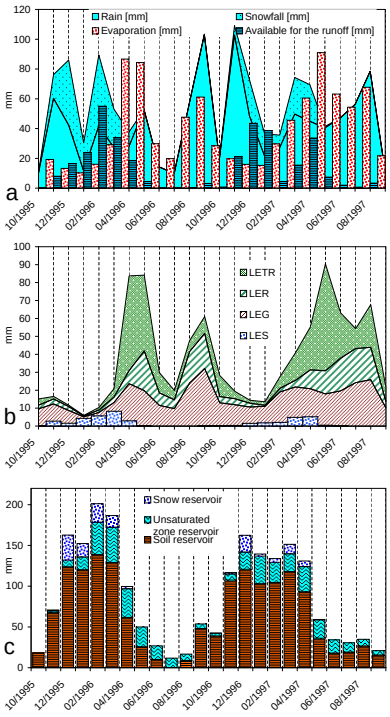

Fig. 11. Monthly evolution of the water budget of the whole basin: **(a)** Main water budget components – Rain and snow precipitations (stacked areas), Total evaporation and Runoff; **(b)** Evaporation components: Bare ground evaporation (*LEG*), Plant transpiration (*LETR*), Intercepted water evaporation (*LER*) and evaporation/sublimation from snow surface (*LES*) (stacked columns representation except *LES*); **(c)** Main water storage reservoirs' evolution: soil reservoir, unsaturated zone reservoir and snow reservoir (stack column representation). The unit for all the variables is mm/year.

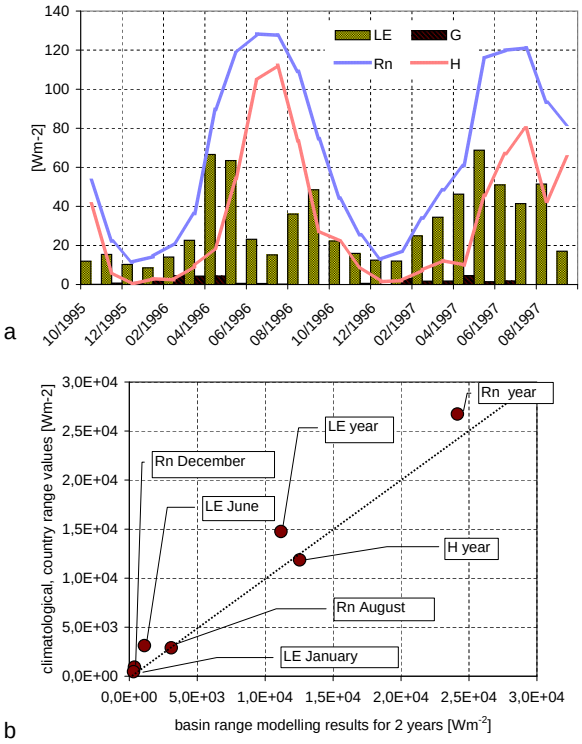

Fig. 12. **(a)** Monthly values of the energy budget for the whole basin: R_n – Net radiation flux [Wm^{-2}], LE – Latent heat flux [Wm^{-2}], H – Sensible heat flux [Wm^{-2}], G – Ground heat flux [Wm^{-2}]; **(b)** Basin-range model energy budget components compared to climatological country-range energy budget components.